Supplemental Data

Reactive Metabolite Induced Protein Glutathionylation Mechanistically Accounts for Acetaminophen Hepatotoxicity

This file includes:

Supplemental Figure S1:	Biochemical analyses of APAP-treated HepaRG cells.
Supplemental Figure S2:	Molecular dynamics simulations of the effects of glutathionylation on VDAC1.
Supplemental Table S1:	Compound-dependent MS parameters for CPT1 assay analytes.
Supplemental Table S2:	Glutathionylation profile of proteins involved in energy metabolism as a function of time.
Supplemental Table S3:	Glutathionylation profile of proteins involved in protein turnover as a function of time.
Supplemental Table S4:	Glutathionylation profile of proteins involved in defense against cellular stress as a function of time.
Supplemental Table S5:	Glutathionylation profile of proteins involved in calcium dynamics and the mitochondrial permeability transition pore formation as a function of time.
Supplemental Table S6:	Summarized reports of APAP-induced metabolic perturbations from literature and in-house data.
Supplemental Table S7:	List of proteins known to be covalently adducted by APAP. Proteins that are also glutathionylated in our dataset are listed in bold.
Supplemental Video 1:	Simulation of open and closed VDAC1 conformations.
Supplemental Video 2	Simulation of enhanced VDAC1 permeability to small molecules and ions following glutathionylation.
Raw peptide data:	0.5 mM APAP_3h_1, 0.5 mM APAP_3h_2, 0.5 mM APAP_3h_3, 0.5 mM APAP+DEDC_3h_1, 0.5 mM APAP+DEDC_3h_2, 0.5 mM APAP+DEDC_3h_3, 30 mM APAP_3h_1, 30 mM APAP_3h_2, 30 mM APAP_3h_3, 30 mM APAP_6h_1, 30 mM APAP_6h_2, 30 mM APAP_6h_3, 30 mM APAP_12h_1, 30 mM APAP_12h_2, 30 mM APAP_12h_3, 30 mM APAP_24h_1, 30 mM

	APAP_24h_2, 30 mM APAP_24h_3, Veh ctrl_1, Veh ctrl_2, Veh ctrl_3, Masterlist of peptide IDs (final).
Processed peptide data:	0.5 mM APAP 3h divided by veh ctrl_HL ratio, 0.5 mM APAP+DEDC 3h divided by veh ctrl_HL ratio, 30 mM APAP 3h divided by veh ctrl_HL ratio, 30 mM APAP 6h divided by veh ctrl_HL ratio, 30 mM APAP 12h divided by veh ctrl_HL ratio, 30 mM APAP 24h divided by veh ctrl_HL ratio, Veh ctrl averaged.

Supplemental References

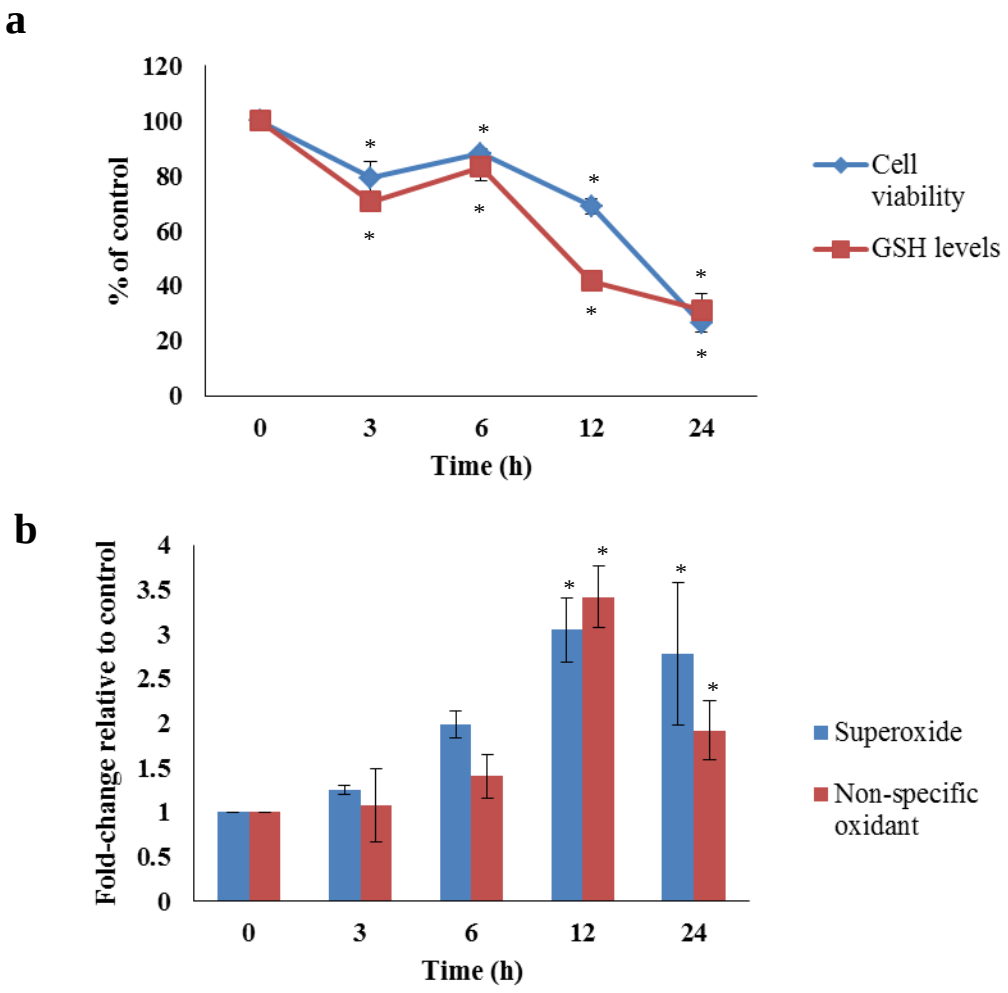

SUPPLEMENTAL FIG. S1. **Biochemical analyses of APAP-treated HepaRG cells.** Time-course of (*A*) cell viability and GSH levels and (*B*) superoxide and non-specific oxidant formation in HepaRG cells exposed to 30 mM APAP over 24 h. * $p < 0.05$ compared to the control. Error bars indicate standard deviations.

a

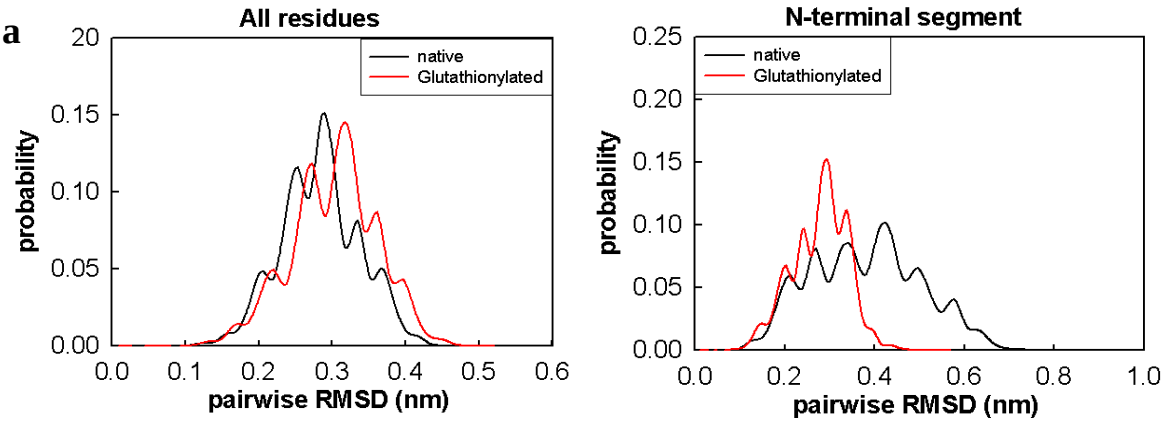
All residues
native
Glutathionylated
probability
pairwise RMSD (nm)
N-terminal segment
native
Glutathionylated
probability
pairwise RMSD (nm)

b

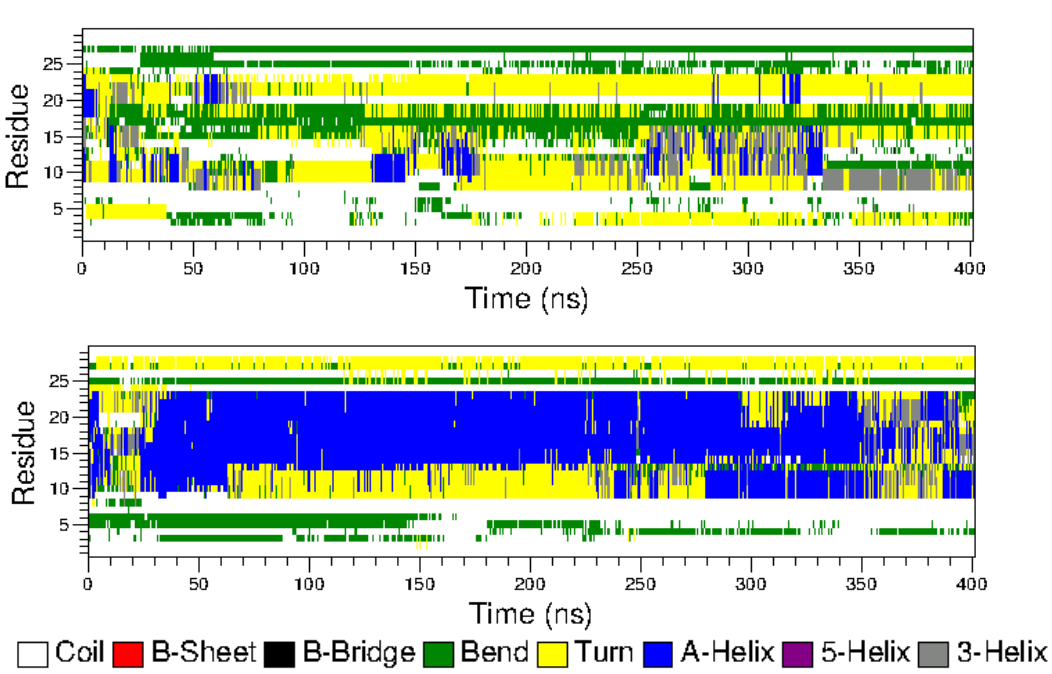
Residue
Time (ns)
Residue
Time (ns)
Coil
B-Sheet
B-Bridge
Bend
Turn
A-Helix
5-Helix
3-Helix

c

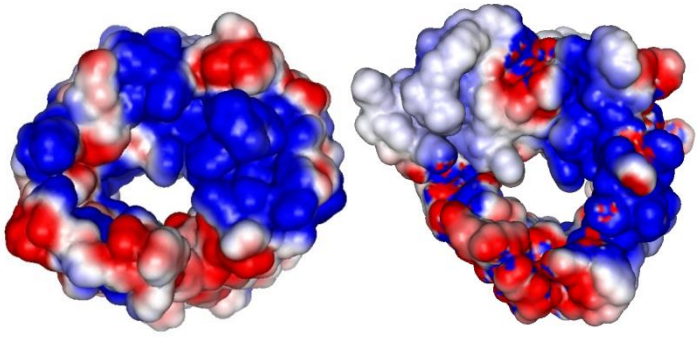

SUPPLEMENTAL FIG. S2. **Molecular dynamics simulations of the effects of glutathionylation on VDAC1.** (*A*) Pairwise RMSD distribution for the whole protein and the N-terminal segment of both native and glutathionylated VDAC1. (*B*) Secondary structure evolution of the N-terminal segment of the native and glutathionylated VDAC1. (*C*) The electrostatic potential map of native (left) and glutathionylated (right) VDAC1. Red region denotes negative electrostatic potential while blue region denotes positive potential.

SUPPLEMENTAL TABLE S1. Compound-dependent MS parameters for CPT1 assay analytes.

Analyte	**MRM Transition (*m/z*)**	**Collision Energy (V)**	**Declustering Potential (V)**	**Entrance Potential (V)**	**Collision Exit Potential (V)**
Palmitoyl carnitine	400 → 85	45	125	12	8
Ketoconazole	531 → 489	44	120	9	11

SUPPLEMENTAL TABLE S2**.** Glutathionylation profile of proteins involved in energy metabolism as a function of time. Values in red represent the average H:L fold-change of peptides normalized to the control that exceed a 1.5-fold threshold across at least 2 replicates.

Pathway	Accession	Description	Gene Symbol	Peptide	H:L fold-change across time (h)			
					3	6	12	24
Glycolysis	P30153	Serine/threonine-protein phosphatase 2A 65 kDa regulatory subunit A alpha isoform	2AAA	EFCENLSADCR	1.35	-	1.14	2.49
				LNIISNLDCVNEVIGIR	1.08	1.71	1.24	0.86
	Q14738	Serine/threonine-protein phosphatase 2A 56 kDa regulatory subunit delta isoform	2A5D	CVSSPHFQVAER	1.70	-	1.12	-
	P04075	Fructose-bisphosphate aldolase A	ALDOA	ALANSLACQGK	1.96	0.79	0.94	1.08
	P60174	Triosephosphate isomerase	TPIS	IAVAAQNCYK	1.76	1.62	0.98	0.84
	P00558	Phosphoglycerate kinase 1	PGK1	ACANPAAGSVILLENLR	1.26	0.89	1.01	36.18
	P06733	Alpha-enolase	ENOA	QIGSVTESLQACK	9.70	7.15	5.49	0.07
	P14618	Pyruvate kinase PKM	KPYM	AAMADTFLEHMCR	0.90	1.60	1.17	0.50
				GIFPVLCK	0.99	1.74	1.07	0.59
				NTGIICTIGPASR	1.65	0.85	0.96	1.08
Import of palmitoyl-CoA into the mitochondrial matrix	O43772	Mitochondrial carnitine/acylcarnitine carrier protein	MCAT	CLLQIQASSGESK	8.76	0.93	1.13	0.99
	P50416	Carnitine O-palmitoyltransferase 1, liver isoform	CPT1A	FCLTYEASMTR	6.17	-	0.04	0.04
Mitochondrial fatty acid β-oxidation	P28330	Long-chain specific acyl-CoA dehydrogenase, mitochondrial	ACADL	AFVDNCLQLHEAK	1.35	1.89	1.41	-
	P49748	Very long-chain specific acyl-CoA dehydrogenase, mitochondrial	ACADV	CLTEPSSGSDAASIR	3.15	3.44	2.47	1.27
				GLQVPSELGGVGLCNTQYAR	2.33	1.21	1.43	1.18
	P55084	Trifunctional enzyme subunit beta, mitochondrial	ECHB	FNNWGGSLSLGHPFGATGCR	3.07	-	2.97	-
	P30084	Enoyl-CoA hydratase, mitochondrial	ECHM	ALNALCDGLIDELNQALK	1.63	0.93	1.06	0.71
	Q16698	2,4-Dienoyl-CoA reductase, mitochondrial	DECR	VHAIQCDVRDPDMVQNTVSELIK	2.12	2.14	2.11	1.16
	P05165	Propionyl-CoA carboxylase alpha chain, mitochondrial	PCCA	MADEAVCVGPAPTSK	2.72	1.39	1.60	0.98
	P05166	Propionyl-CoA carboxylase beta chain, mitochondrial	PCCB	AFENDVDALCNLR	5.56	5.62	-	-
				CADFGMAADK	1.74	0.99	0.87	1.42
	Q96PE7	Methylmalonyl-CoA epimerase, mitochondrial	MCEE	DCGGVLVELEQA	85.5	-	1.00	-
Pyruvate metabolism	P09622	Dihydrolipoyl dehydrogenase, mitochondrial	DLDH	ILGPGAGEMVNEAALALEYGAS CEDIAR	3.26	2.92	2.64	-

Pathway	Accession	Description	Gene Symbol	Peptide	H:L fold-change across time (h)			
					3	6	12	24
	P08559	Pyruvate dehydrogenase E1 component subunit alpha, somatic form, mitochondrial	ODPA	VDGMDILCVR	2.74	1.24	1.60	1.05
	P10515	Dihydrolipoyllysine-residue acetyltransferase component of pyruvate dehydrogenase complex, mitochondrial	ODP2	ASALACLK	2.73	2.58	1.13	0.51
Citric acid cycle	O75390	Citrate synthase, mitochondrial	CISY	LPCVAAK	5.94	1.28	1.46	1.79
	Q99798	Aconitate hydratase, mitochondrial	ACON	CTTDHISAAGPWLK	1.63	1.45	1.38	0.85
	P51553	Isocitrate dehydrogenase [NAD] subunit gamma, mitochondrial	IDH3G	HACVPVDFEEVHVSSNADEEDIR	1.11	1.59	0.94	1.03
				LGDGLFLQCCR	1.94	-	-	-
	P48735	Isocitrate dehydrogenase [NADP], mitochondrial	IDHP	DLAGCIHGLSNVK	1.34	1.87	1.46	1.24
	P50213	Isocitrate dehydrogenase [NAD] subunit alpha, mitochondrial	IDH3A	CSDFTEEICR	1.93	0.03	0.99	2.04
	Q02218	2-Oxoglutarate dehydrogenase, mitochondrial	ODO1	DVVVDLVCYR	1.90	3.06	1.18	1.27
				CSTPGNFFHVLR	3.62	-	-	-
	P09622	Dihydrolipoyl dehydrogenase, mitochondrial	DLDH	ILGPGAGEMVNEAALALEYGAS CEDIAR	3.26	2.92	2.64	-
	P53597	Succinyl-CoA ligase [ADP/GDP-forming] subunit alpha, mitochondrial	SUCA	IICQGFTGK	1.30	1.00	1.19	2.47
				LIGPNCPGVINPGECK	1.63	-	1.09	0.29
	P31040	Succinate dehydrogenase [ubiquinone] flavoprotein subunit, mitochondrial	SDHA	GLSEAGFNTACVTK	1.86	-	1.73	1.15
				GVIALCIEDGSIHR	1.23	1.78	1.00	0.37
	P21912	Succinate dehydrogenase [ubiquinone] iron-sulfur subunit, mitochondrial	SDHB	CGPMVLDALIK	2.24	3.92	1.85	0.82
	Q99643	Succinate dehydrogenase cytochrome b560 subunit, mitochondrial	C560	SLCLGPALIHTAK	1.21	2.46	1.68	1.06
	P40926	Malate dehydrogenase, mitochondrial	MDHM	GCDVVVIPAGVPR	2.49	1.33	1.14	1.30
Respiratory electron transport, ATP synthesis	P28331	NADH-ubiquinone oxidoreductase 75 kDa subunit, mitochondrial	NDUS1	DCFIIYQGHHGDVGAPIADVILPG AAYTEK	1.85	1.14	-	1.26
	O95299	NADH dehydrogenase [ubiquinone] 1 alpha subcomplex subunit 10, mitochondrial	NDUAA	CEVLQYSAR	2.32	-	1.29	-
	P49821	NADH dehydrogenase [ubiquinone] flavoprotein 1, mitochondrial	NDUV1	GAGAYICGEETALIESIEGK	1.99	1.94	8.73	-
	P31040	Succinate dehydrogenase [ubiquinone] flavoprotein subunit, mitochondrial	SDHA	GLSEAGFNTACVTK	1.86	-	1.73	1.15
				GVIALCIEDGSIHR	1.23	1.78	1.00	0.37
	P21912	Succinate dehydrogenase [ubiquinone] iron-sulfur subunit, mitochondrial	SDHB	CGPMVLDALIK	2.24	3.92	1.85	0.82

Pathway	Accession	Description	Gene Symbol	Peptide	H:L fold-change across time (h)			
					3	6	12	24
	Q99643	Succinate dehydrogenase cytochrome b560 subunit, mitochondrial	C560	SLCLGPALIHTAK	1.21	2.46	1.68	1.06
	P31930	Cytochrome b-c1 complex subunit 1, mitochondrial	QCR1	NALVSHLDGTTPVCEDIGR	1.38	1.00	1.22	2.12
				SICYAETGLLGAHFVCDR	5.21	-	1.44	0.93
	P22695	Cytochrome b-c1 complex subunit 2, mitochondrial	QCR2	ENMAYTVECLR	2.53	2.34	2.00	2.55
				NALANPLYCPDYR	2.98	1.25	1.20	5.83
	P08574	Cytochrome c1, heme protein, mitochondrial	CY1	HLVGVCYTEDEAK	1.16	1.88	0.78	0.43
	P24539	ATP synthase F(0) complex subunit B1, mitochondrial	AT5F1	CIADLK	1.88	1.47	1.39	-
	P13804	Electron transfer flavoprotein subunit alpha, mitochondrial	ETFA	LGGEVSCLVAGTK	0.94	1.03	1.45	2.98
				TIYAGNALCTVK	3.90	1.20	2.59	1.32
	P38117	Electron transfer flavoprotein subunit beta	ETFB	HSMNPFCEIAVEEAVR	1.26	1.34	1.39	2.09
	Q16134	Electron transfer flavoprotein-ubiquinone oxidoreductase, mitochondrial	ETFD	QNVAVNELCGR	1.25	8.49	1.23	-
				FCPAGVYEFVPVEQGDGFR	105	131	117	137
	P42704	Leucine-rich PPR motif-containing protein, mitochondrial	LPPRC	LEDVALQILLACPVSK	1.05	1.89	1.63	1.38
				LIASYCNVGDIEGASK	1.61	1.10	1.33	1.18
Gluconeogenesis	P00505	Aspartate aminotransferase, mitochondrial	AATM	TCGFDFTGAVEDISK	2.88	1.02	0.95	0.48
				VGAFTMVCK	2.20	1.17	0.66	0.70
				ACANPAAGSVILLENLR	1.26	0.89	1.01	36.18
	Q16822	Phosphoenolpyruvate carboxykinase [GTP], mitochondrial	PCKGM	YVAAAFPSACGK	0.99	1.17	1.83	3.21
	P40925	Malate dehydrogenase, cytoplasmic	MDHC	MGVLDGVLMELQDCALPLLK	7.25	-	6.29	-
				GCDVVVIPAGVPR	2.49	1.33	1.14	1.30
	P04075	Fructose-bisphosphate aldolase A	ALDOA	ALANSLACQGK	1.96	0.79	0.94	1.08
	P06733	Alpha-enolase	ENOA	QIGSVTESLQACK	9.70	7.15	5.49	0.07
	P00558	Phosphoglycerate kinase 1	PGK1	ACANPAAGSVILLENLR	1.26	0.89	1.01	36.18
	P11498	Pyruvate carboxylase, mitochondrial	PYC	GLYAAFDCTATMK	4.96	3.14	3.48	4.84
	P53007	Tricarboxylate transport protein, mitochondrial	TXTP	GIGDCVR	1.48	1.59	1.14	0.80
	P40926	Malate dehydrogenase, mitochondrial	MDHM	GCDVVVIPAGVPR	2.49	1.33	1.14	1.30
	P60174	Triosephosphate isomerase	TPIS	IAVAAQNCYK	1.76	1.62	0.98	0.84
Pentose phosphate pathway	P11413	Glucose-6-phosphate 1-dehydrogenase	G6PD	DNIACVILTFK	3.47	1.96	1.27	0.84
				DVMQNHLLQMLCL	2.88	1.26	1.01	1.45
				LILDVFCGSQMHF	2.33	1.09	1.34	0.92
	P52209	6-Phosphogluconate dehydrogenase, decarboxylating	6PGD	MVHNGIEYGDMQLICEAYHLMK	6.29	-	9.79	-
				SAVENCQDSWR	1.77	2.05	1.50	0.97

Pathway	Accession	Description	Gene Symbol	Peptide	H:L fold-change across time (h)			
					3	6	12	24
	P29401	Transketolase	TKT	CSTFAAFFTR	2.24	0.98	1.06	1.31
				AIIVDGHSVEELCK	1.92	3.77	1.18	0.68
	P37837	Transaldolase	TALDO	ALAGCDFLTISPK	1.76	2.10	1.10	0.66
Fatty acyl-CoA biosynthesis	P49327	Fatty acid synthase	FAS	AALQEELQLCK	1.09	1.82	1.14	2.34
				AAPLDSIHSLAAYYIDCIR	3.06	4.64	2.65	2.78
				ACLDTAVENMPSLK	15.8	5.37	0.98	1.21
				AINCATSGVVGLVNCLR	4.68	0.09	0.48	0.09
				CTVFHGAQVEDAFR	1.72	1.54	1.16	0.96
				LSIPTYGLQCTR	2.79	1.30	0.95	1.41
				MASCLEVLDLFLNQPH	1.53	3.60	1.15	1.18
				SFYGSTLFLCR	1.06	1.52	0.98	1.31
				TGGAYGEDLGADYNLSQVCDGK	2.85	2.07	2.40	0.04
	P33121	Long-chain-fatty-acid--CoA ligase 1	ACSL1	AAEGEGEVCVK	1.17	1.35	1.14	1.94
				CGVEVTSMK	1.73	1.02	1.22	1.95
				GFEGSFEELCR	2.12	2.16	1.39	1.31
				GIQVSNNGPCLGSR	2.61	1.39	1.33	3.57
				LIAIVVPDVETLCSWAQK	2.42	3.07	1.59	1.24
	O95573	Long-chain-fatty-acid--CoA ligase 3	ACSL3	NTPLCDSFVFR	3.30	1.36	1.21	1.48
	O60488	Long-chain-fatty-acid--CoA ligase 4	ACSL4	TALLDISCVK	1.12	1.63	1.39	1.39
	Q9ULC5	Long-chain-fatty-acid--CoA ligase 5	ACSL5	GLAVSDNGPCLGYR	1.14	1.09	1.65	2.39
				IVQAVVYSCGAR	1.40	1.43	1.37	2.38
	P53396	ATP-citrate synthase	ACLY	AVQGMLDFDYVCSR	1.02	1.13	1.26	1.86
				FICTTSAIQNR	2.11	1.45	1.57	-
	P53007	Tricarboxylate transport protein, mitochondrial	TXTP	GIGDCVR	1.48	1.59	1.14	0.80
	Q53GQ0	Very-long-chain 3-oxoacyl-CoA reductase	DHB12	MININILSVCK	1.52	2.32	1.80	0.46

N.B. '-' denotes not detected in at least 2 of 3 replicates

SUPPLEMENTAL TABLE S3. Glutathionylation profile of proteins involved in protein turnover as a function of time. Values in red represent the average H:L ratio of peptides normalized to the control that exceed a 1.5-fold threshold across at least 2 replicates.

Pathway	Accession	Description	Gene Symbol	Peptide	H:L fold-change across time (h)			
					3	6	12	24
Amino acid metabolism	Q9UDR5	Alpha-aminoadipic semialdehyde synthase, mitochondrial	AASS	AGGILQEDISEACLILGVK	1.05	1.65	1.13	0.72
				QLLCDLVGISPSSEHDVLK	1.08	4.00	0.86	1.34
	P35520	Cystathionine beta-synthase	CBS	CIIVMPEK	1.69	-	-	-
	Q14353	Guanidinoacetate N-methyltransferase	GAMT	TEVMALVPPADCR	1.29	-	1.21	2.72
	P30038	Delta-1-pyrroline-5-carboxylate dehydrogenase, mitochondrial	AL4A1	CDDSVGYFVEPCIVESK	3.29	-	1.83	2.55
	P31327	Carbamoyl-phosphate synthase [ammonia], mitochondrial	CPSM	SAYALGGLGSGICPNR	1.68	0.98	1.17	-
	P23526	Adenosylhomocysteinase	SAHH	QAQYLGMSCDGPFKPDHYR	5.12	-	-	-
	O15382	Branched-chain-amino-acid aminotransferase, mitochondrial	BCAT2	EVFGSGTACQVCPVHR	8.21	-	-	-
				LCLPSFDK	13.63	1.06	1.27	1.14
				LELLECIR	12.00	4.60	2.40	0.90
	Q9UBQ7	Glyoxylate reductase/hydroxypyruvate reductase	GRHPR	GVAGAHGLLCLLSDHVDK	1.28	2.27	1.39	1.13
				NCVILPH	1.58	1.08	1.33	1.14
	P09622	Dihydrolipoyl dehydrogenase, mitochondrial	DLDH	ILGPGAGEMVNEAALALEYGAS CEDIAR	3.26	2.92	2.64	-
	P19623	Spermidine synthase	SPEE	QFCQSLFPVVAY	1.81	-	-	-
	P00505	Aspartate aminotransferase, mitochondrial	AATM	TCGFDFTGAVEDISK	2.88	1.02	0.95	0.48
				VGAFTMVCK	2.20	1.17	0.66	0.70
	P21953	2-oxoisovalerate dehydrogenase subunit beta, mitochondrial	ODBB	GLLLSCIEDK	1.92	2.23	1.25	-
	P34896	Serine hydroxymethyltransferase, cytosolic	GLYC	YYGGAEVVDEIELLCQR	2.09	1.39	1.71	1.40
	Q02218	2-oxoglutarate dehydrogenase, mitochondrial	ODO1	DVVVDLVCYR	1.90	3.06	1.18	1.27
				CSTPGNFFHVLR	3.62	-	-	-
	P04424	Argininosuccinate lyase	ARLY	CAGLLMTLK	3.12	-	1.47	-
				MAEDLILYCTK	4.71	3.25	1.50	2.96
	P49189	4-trimethylaminobutyraldehyde dehydrogenase	AL9A1	SPLIIFSDCDMNNAVK	1.58	1.15	1.12	1.20
	P48506	Glutamate--cysteine ligase catalytic subunit	GSH1	GYVSDIDCR	104	44.4	46.1	1.00
	P31937	3-hydroxyisobutyrate dehydrogenase, mitochondrial	3HIDH	HGYPLIIYDVFPDACK	2.02	1.05	1.06	0.90

Pathway	Accession	Description	Gene Symbol	Peptide	H:L fold-change across time (h)			
					3	6	12	24
	P25398	40S ribosomal protein S12	RS12	LVEALCAEHQINLIK	1.37	2.89	1.27	1.00
				QAHLCVLASNCDEPMYVK	3.41	-	1.30	1.4
	P23396	40S ribosomal protein S3	RS3	ACYGVLR	1.90	1.17	1.26	1.09
				GCEVVVSGK	1.81	1.93	1.27	1.24
				GLCAIAQAESLR	2.22	1.19	3.21	3.25
Eukaryotic translation initiation, elongation, termination	P61247	40S ribosomal protein S3a	RS3A	LFCVGF	2.31	4.25	1.41	-
	P62241	40S ribosomal protein S8	RS8	NCIVLIDSTPYR	1.37	2.46	1.07	0.77
	P05388	60S acidic ribosomal protein P0	RLA0	AGAIAPCEVTVPAQNTGLGPEK	2.22	0.93	1.38	2.13
				CFIVGADNVGSK	1.8	0.58	0.84	0.50
				NVASVCLQIGYPTVASVPH	3.03	1.20	1.63	0.94
	P62906	60S ribosomal protein L10a	RL10A	VLCLAVAVGH	4.01	-	1.36	-
				VLCLAVAVGHVK	3.23	-	0.59	-
	P30050	60S ribosomal protein L12	RL12	CTGGEVGATSALAPK	3.43	1.53	1.32	0.55
	P39023	60S ribosomal protein L3	RL3	TVFAEHISDECK	1.39	1.09	1.62	1.28
				VACIGAWHPAR	1.94	0.97	2.48	-
				YCQVIR	2.26	0.94	-	-
	P62910	60S ribosomal protein L32	RL32	ELEVLLMCNK	1.70	1.34	1.37	1.32
	P36578	60S ribosomal protein L4	RL4	GPCIIYNEDNGIIK	1.37	0.82	1.88	1.01
				SGQGAFGNMCR	1.73	-	1.56	1.94
	P46777	60S ribosomal protein L5	RL5	AAAYCTGLLLAR	1.64	0.82	1.11	1.48
				DIICQIAY	2.33	0.79	1.48	0.85
				IEGDMIVCAAYAHELPK	2.61	2.32	1.56	0.88
				VGLTNYAAAYCTGLLLAR	2.09	2.02	-	-
	Q01518	Adenylyl cyclase-associated protein 1	CAP1	CVNTTLQIK	2.07	0.79	1.08	0.35
				INSITVDNCK	1.49	1.8	1.07	0.41
	P12814	Alpha-actinin-1	ACTN1	CQLEINFNTLQTK	92.6	6.89	11.6	5.18
				DGLGFCALIHR	0.99	2.19	0.65	0.03
				EGLLLWCQR	0.94	1.76	0.89	1.03
	P23528	Cofilin-1	COF1	HELQANCYEEVKDR	2.15	1.20	1.00	0.92
	P68104	Elongation factor 1-alpha 1	EF1A1	DGNASGTTLLEALDCILPPTRPTDKPLR	1.49	2.33	1.21	0.77

Pathway	Accession	Description	Gene Symbol	Peptide	H:L fold-change across time (h)			
					3	6	12	24
				SGDAAIVDMVPGKPMCVESFSDYPPLGR	0.92	54.0	3.38	1.35
	P13639	Elongation factor 2	EF2	CLYASVLTAQPR	2.75	1.39	1.1	0.67
				STLTDSLVCK	1.09	0.44	0.68	1.80
				YVEPIEDVPCGNIVGLVGVDQFLVK	0.24	0.08	0.72	2.00
	P60842	Eukaryotic initiation factor 4A-I	IF4A1	VVMALGDYMGASCHACIGGTNVR	2.81	-	-	-
	P62495	Eukaryotic peptide chain release factor subunit 1	ERF1	CGTIVTEEGK	2.83	-	-	-
	P47813	Eukaryotic translation initiation factor 1A, X-chromosomal	IF1AX	LEAMCFDGVK	1.69	-	1.30	0.02
	P41091	Eukaryotic translation initiation factor 2 subunit 3	IF2G	YNIEVVCEYIVK	1.92	-	0.90	-
	P55884	Eukaryotic translation initiation factor 3 subunit B	EIF3B	NLFNVVDCK	2.79	2.16	2.09	2.25
	P60228	Eukaryotic translation initiation factor 3 subunit E	EIF3E	IHQCISIN	1.42	1.10	1.15	2.86
				LFIFETFCR	2.23	-	2.43	-
	O75822	Eukaryotic translation initiation factor 3 subunit J	EIF3J	ITNSLTVLCSEK	6.16	2.03	1.33	0.82
	Q9UBQ5	Eukaryotic translation initiation factor 3 subunit K	EIF3K	FICHVVGITYQHIDR	2.08	-	1.35	-
	P02675	Fibrinogen beta chain	FIBB	ECEEIIR	1.63	2.09	-	-
				LESDVSAQMEYCR	0.78	3.33	3.75	3.43
				TPCTVSCNIPVVSGK	2.91	5.05	3.56	1.08
	P02679	Fibrinogen gamma chain	FIBG	CHAGHLNGVYYQGGTYSK	0.80	1.60	2.09	2.13
				VAQLEAQCQEPCKDTVQIHDITGK	3.74	5.77	4.55	0.87
	P21333	Filamin-A	FLNA	VHSPSGALEECYVTEIDQDK	2.25	1.42	1.59	0.02
	P04075	Fructose-bisphosphate aldolase A	ALDOA	ALANSLACQGK	1.96	0.79	0.94	1.08
	P62937	Peptidyl-prolyl cis-trans isomerase A	PPIA	ANAGPNTNGSQFFICTAK	4.72	3.88	3.80	0.06
				TNGSQFFICTAK	1.56	0.78	0.84	1.21
	P07737	Profilin-1	PROF1	CYEMASHLR	1.99	1.60	1.06	-
				IDNLMADGTCQDAAIVGYK	3.37	-	4.21	-

Pathway	Accession	Description	Gene Symbol	Peptide	H:L fold-change across time (h)			
					3	6	12	24
	Q12846	Syntaxin-4	STX4	CNSMQSEYR	1.69	-	-	-
	O75083	WD repeat-containing protein 1	WDR1	MTVDESGQLISCSMDDTVR	12.4	2.10	0.27	1.18
	Q9BVA1	Tubulin beta-2B chain	TBB2B	LTTPTYGDLNHLVSATMSGVTT CLR	1.66	-	-	-
	Q9BQE3	Tubulin alpha-1C chain	TBA1C	AVCMLSNTTAVAEAWAR	0.91	-	0.73	1.74
				LADQCTGLQGFLVFHSF	1.34	-	10.9	1.47
				MVDNEAIYDICR	10.9	10.6	10.7	8.46
				TTLEHSDCAFMVDNEAIYDICR	1.47	1.77	1.03	-
	P68363	Tubulin alpha-1B chain	TBA1B	AYHEQLSVAEITNACFEPANQM VK	1.36	1.25	1.97	1.14
				LADQCTGLQGF	1.58	-	1.26	0.74
				TTLEHSDCAFMVDNEAIYDICR	2.03	-	1.22	0.93
				YMACCLLYR	1.99	-	1.44	3.17
Protein folding	P50991	T-complex protein 1 subunit delta	TCPD	SIHDALCVIR	1.65	2.21	1.24	0.49
	P50990	T-complex protein 1 subunit theta	TCPQ	IGLSVSEVIEGYEIACR	1.63	1.70	0.89	0.43
	P68366	Tubulin alpha-4A chain	TBA4A	AYHEQLSVAEITNACFEPANQM VK	1.36	1.13	1.69	1.14
				MVDNEAIYDICR	12.0	10.6	10.33	8.46
				SIQFVDWCPTGF	6.53	-	7.97	-
				TTLEHSDCAFMVDNEAIYDICR	1.47	1.77	1.03	-
				YMACCLLYR	1.99	-	1.44	3.17
	P48643	T-complex protein 1 subunit epsilon	TCPE	SLHDALCVIR	1.70	2.21	1.24	0.49
	P17987	T-complex protein 1 subunit alpha	TCPA	ALNCVVGSQGMPK	2.11	-	1.34	1.01
				GANDFMCDEMER	3.35	1.95	2.66	2.29
				IACLDFSLQK	3.11	3.28	1.22	1.05
				ICDDELILIK	0.98	1.51	1.24	0.93
	P60709	Actin, cytoplasmic 1	ACTB	DDDIAALVVDNGSGMCK	25.71	0.76	27.24	1.39
	Q92890	Ubiquitin fusion degradation protein 1 homolog	UFD1	CFSVSMLAGPNDR	99.7	-	-	-
	P61086	Ubiquitin-conjugating enzyme E2 K	UBE2K	ISSVTGAICLDILK	15.1	-	-	-
Protein degradation	P49792	E3 SUMO-protein ligase RanBP2	RBP2	IAELLCK	2.41	1.17	1.29	-
	Q14258	E3 ubiquitin/ISG15 ligase TRIM25	TRI25	NTVLCNVVEQFLQADLAR	2.74	-	44.7	-
	Q7Z6Z7	E3 ubiquitin-protein ligase HUWE1	HUWE1	VLGPAACR	1.66	1.21	1.26	-

Pathway	Accession	Description	Gene Symbol	Peptide	H:L fold-change across time (h)			
					3	6	12	24
	Q63HN8	E3 ubiquitin-protein ligase RNF213	RN213	STDFLPVDCPVR	1.70	-	-	-
	P62333	26S protease regulatory subunit 10B	PRS10	AVASQLDCNFLK	3.05	1.30	13.36	1.21
	Q99460	26S proteasome non-ATPase regulatory subunit 1	PSMD1	QCVENADLPEGEK	1.83	3.58	1.86	0.70
			PSMD1	MEEADALIESLCR	1.27	1.90	0.74	-
	O00232	26S proteasome non-ATPase regulatory subunit 12	PSD12	AIYDTPCIQAESEK	23.3	1.14	2.18	1.80
	Q9UNM6	26S proteasome non-ATPase regulatory subunit 13	PSD13	FLGCVDIK	1.30	1.80	1.15	0.81
	Q16401	26S proteasome non-ATPase regulatory subunit 5	PSMD5	FFGNLAVMDSPQQICER	108	-	-	-
			PSMD5	TTLCVSILER	1.76	-	-	-
	Q15008	26S proteasome non-ATPase regulatory subunit 6	PSMD6	VYQGLYCVAIR	1.79	0.61	1.03	0.02

N.B. '-' denotes not detected in at least 2 of 3 replicates

SUPPLEMENTAL TABLE S4. Glutathionylation profile of proteins involved in defense against cellular stress as a function of time. Values in red represent the average H:L ratio of peptides normalized to the control that exceed a 1.5-fold threshold across at least 2 replicates.

Pathway	Accession	Description	Gene Symbol	Peptide	H:L fold-change across time (h)			
					3	6	12	24
Detoxification of reactive oxygen species	P04040	Catalase	CATA	LCENIAGHLK	3.04	1.05	1.19	0.34
	P30048	Thioredoxin-dependent peroxide reductase, mitochondrial	PRDX3	ANEFHDVNCEVVAVSVDSHFSH LAWINTPR	5.49	-	4.02	-
	P00441	Superoxide dismutase [Cu-Zn]	SODC	HVGDLGNVTADKDGVADVSIED SVISLSGDHCIIGR	1.22	1.63	1.81	-
	P04179	Superoxide dismutase [Mn], mitochondrial	SODM	GHLQIAACPNQDPLQGTTGLIPL LGID	83.76	-	-	-
	Q96HE7	ERO1-like protein alpha	ERO1A	YSEEANNLIEECEQAER	0.97	0.94	1.94	1.34
	Q06830	Peroxiredoxin-1	PRDX1	LNCQVIGASVDSHFCH	0.98	-	3.43	-
Phase I functionalization	P21397	Amine oxidase [flavin-containing] A	AOFA	ICELYAK	2.23	2.13	1.33	0.58
	P27338	Amine oxidase [flavin-containing] B	AOFB	CIVYYK	3.03	-	1.21	-
				LCELYAK	2.12	2.13	1.33	0.58
	P07327	Alcohol dehydrogenase 1A	ADH1A	NPESNYCLK	300	150	-	-
	P00325	Alcohol dehydrogenase 1B	ADH1B	MVAVGICR	5.66	2.55	1.81	1.14
				NPESNYCLK	335	131	115	1.00
	P00326	Alcohol dehydrogenase 1C	ADH1G	NPESNYCLK	333	-	-	-
	P05181	Cytochrome P450 2E1	CP2E1	DLTDCLLVEMEK	2.70	51.58	3.90	-
	P10632	Cytochrome P450 2C8	CP2C8	DFIDCFLIK	3.01	0.96	1.27	1.31
	P00352	Retinal dehydrogenase 1	AL1A1	AYLNDLAGCIK	2.19	1.00	1.00	1.16
				FPVFNPATEEELCQVEEGDKEDV DK	236	164	68.7	-
				LECGGGPWGNK	4.95	2.69	1.33	-
				LNDLAGCIK	2.70	1.43	1.11	0.88
				YCAGWADK	2.73	1.29	0.91	1.10
	Q9NR19	Acetyl-coenzyme A synthetase, cytoplasmic	ACSA	GATTNICYNVLDR	1.83	72.98	1.22	2.27
	Q16850	Lanosterol 14-alpha demethylase	CP51A	CIGENFAYVQIK	1.07	1.07	1.48	2.41
	Q9HBI6	Phylloquinone omega-hydroxylase CYP4F11	CP4FB	LQCFPQPPK	1.32	1.27	1.10	2.76
Phase II conjugation	P10620	Microsomal glutathione S-transferase 1	MGST1	VFANPEDCVAFGK	4.95	2.94	2.97	12.16

Pathway	Accession	Description	Gene Symbol	Peptide	H:L fold-change across time (h)			
					3	6	12	24
	P40261	Nicotinamide N-methyltransferase	NNMT	IFCLDGVK	2.45	3.18	1.35	0.89
	P48506	Glutamate--cysteine ligase catalytic subunit	GSH1	GYVSDIDCR	104	44.4	46.1	1.00
	P36269	Gamma-glutamyltransferase 5	GGT5	FLNVVQAVSQEGACVYAVSDLR	2.78	39.8	-	-
				HQAPCGPQAF	1.17	0.69	2.38	-
	P48637	Glutathione synthetase	GSHB	IEPEPFENCLLR	4.70	-	-	-
	P23526	Adenosylhomocysteinase	SAHH	QAQYLGMSCDGPFKPDHYR	5.12	-	-	-
	P51580	Thiopurine S-methyltransferase	TPMT	SWGIDCLFEK	2.74	-	-	-
	O60701	UDP-glucose 6-dehydrogenase	UGDH	DPYEACDGAH	0.88	1.10	1.59	1.00
				DVLNLVYLCEALNLPEVAR	4.65	4.50	1.45	1.07
	O60656	UDP-glucuronosyltransferase 1-9	UD19	NHIMHLEEHLLCHR	6.40	-	1.09	0.59
	Q06520	Bile salt sulfotransferase	ST2A1	ICQFLGK	1.00	0.92	1.24	2.13
GSH and sulfur amino acid metabolism	P35520	Cystathionine beta-synthase	CBS	CIIVMPEK	1.69	-	-	-
	P23526	Adenosylhomocysteinase	SAHH	QAQYLGMSCDGPFKPDHYR	5.12	4.33	-	-
	P48506	Glutamate--cysteine ligase catalytic subunit	GSH1	GYVSDIDCR	104	44.4	46.1	1.00
	P48637	Glutathione synthetase	GSHB	IEPEPFENCLLR	4.70	-	-	-
	P19623	Spermidine synthase	SPEE	QFCQSLFPVVAY	1.81	-	-	-
	P52788	Spermine synthase	SPSY	LYCPVEFSK	2.55	-	-	-
Cellular response to heat stress	O95816	BAG family molecular chaperone regulator 2	BAG2	FQSIVIGCALEDQK	2.37	-	0.85	0.84
	Q8N163	Cell cycle and apoptosis regulator protein 2	CCAR2	GEASEDLCEMALDPELLLLR	2.64	-	4.49	-
				TVDSPICDFLELQR	1.97	-	1.47	1.61
	Q15185	Prostaglandin E synthase 3	TEBP	LTFSCLGGSDNFK	1.73	1.92	2.69	3.31
	P68104	Elongation factor 1-alpha 1	EF1A1	DGNASGTTLLEALDCILPPTRPTDKPLR	1.49	2.33	1.21	0.77
				SGDAAIVDMVPGKPMCVESFSDYPPLGR	0.92	54.0	3.38	1.35
	P49792	E3 SUMO-protein ligase RanBP2	RBP2	IAELLCK	2.41	1.17	1.29	-
	Q8N1F7	Nuclear pore complex protein Nup93	NUP93	CGDLLAASQVVNR	1.61	1.26	1.15	1.41
	P34932	Heat shock 70 kDa protein 4	HSP74	FLEMCNDLLAR	0.98	2.71	1.01	-
	O95757	Heat shock 70 kDa protein 4L	HS74L	AQFEQLCASLLAR	3.14	3.04	1.23	-
	P08107	Heat shock 70 kDa protein 1A/1B	HSP71	CQEVISWLDANTLAEKDEFEHK	5.07	-	-	-
	P11142	Heat shock cognate 71 kDa protein	HSP7C	CNEIINWLDK	1.15	3.82	1.00	1.78

Pathway	Accession	Description	Gene Symbol	Peptide	H:L fold-change across time (h)			
					3	6	12	24
	P07900	Heat shock protein HSP 90-alpha	HS90A	CLELFTELAEDK	0.91	1.63	0.33	-
				FENLCK	3.66	-	-	-
	P08238	Heat shock protein HSP 90-beta	HS90B	AKFENLCK	1.58	-	-	-
				FENLCK	3.60	-	-	-
				VFIMDSCDELIPEYLNFIR	67.5	34.3	79.2	50.3
	P55072	Transitional endoplasmic reticulum ATPase	TERA	EAVCIVLSDDTCSDEK	59.4	-	40.2	-
				LADDVDLEQVANETHGHVGADL AALCSEAALQAIR	91.9	281	64.0	37.6

N.B. '-' denotes not detected in at least 2 of 3 replicates

SUPPLEMENTAL TABLE S5 Glutathionylation profile of proteins involved in calcium dynamics and the mitochondrial permeability transition pore formation as a function of time. Values in red represent the average H:L ratio of peptides normalized to the control that exceed a 1.5-fold threshold across at least 2 replicates.

Pathway	Accession	Description	Gene Symbol	Peptide	H:L fold-change across time (h)			
					3	6	12	24
Calcium dynamics	P16615	Sarcoplasmic/endoplasmic reticulum calcium ATPase 2	AT2A2	ANACNSVIK	-	1.24	-	1.68
				GTAVAICR	2.32	1.30	1.18	1.35
	P20020	Plasma membrane calcium-transporting ATPase 1	AT2B1	TICLAFR	5.00	-	1.10	-
Mitochondrial permeability transition pore formation	P21796	Voltage-dependent anion-selective channel protein 1	VDAC1	YQIDPDACFSAK	1.67	0.99	1.28	0.88
	P45880	Voltage-dependent anion-selective channel protein 2	VDAC2	SCSGVEFSTSGSSNTDTGK	1.26	0.81	1.32	2.58
	Q9Y277	Voltage-dependent anion-selective channel protein 3	VDAC3	SCSGVEFSTSGHAYTDTGK	0.87	0.83	1.68	1.84
				VCNYGLTFTQK	0.97	0.96	1.68	2.50
	P12235/ P05141	ADP/ATP translocase 1/2	ADT1/ ADT2	QYKGIIDCVVR	3.42	2.64	1.18	1.15
	P62937	Peptidyl-prolyl cis-trans isomerase A	PPIA	ANAGPNTNGSQFFICTAK	4.72	3.88	3.80	0.06

N.B. '-' denotes not detected in at least 2 of 3 replicates

SUPPLEMENTAL TABLE S6. Summarized reports of APAP-induced metabolic perturbations from literature and in-house data.

Pathway	Model system	Matrix	Analytical platform	Metabolites	Directionality	Ref
Glycolysis, pyruvate metabolism	Mouse	Plasma	NMR	Lactate	Elevated	(12)
		Liver		Lactate	Elevated	
	Rat	Urine	NMR	Lactate	Elevated	(13)
	Human	Plasma	NMR	Lactate	Elevated	(14)
	Human	Serum	NMR	Lactate	Elevated	(15)
	Mouse	Plasma	NMR	Pyruvate	Elevated	(12)
	Rat	Plasma	NMR	Pyruvate	Elevated	(13)
	Rat	Urine	NMR, LC/MS	Pyruvate	Decreased	(16)
	Rat	Liver	CE/TOFMS	Phosphoenolpyruvate	Elevated	(17)
Mitochondrial fatty acid β-oxidation	Mouse	Serum	LC/MS	Palmitoyl, oleoyl, myristoylcarnitine	Peak at 4 h followed by decline	(18)
				Carnitine	Peak at 8 h followed by decline	
				Acetylcarnitine	Decreased	
	Mouse	Plasma	LC/MS	Palmitoyl, oleoyl, myristoyl, palmitoleoyl carnitine	Peak at 2 h followed by decline	(19)
	Mouse	Serum	LC/MS	Palmitoyl, linoleoyl, oleoyl carnitine	Elevated from 3-12 h	(20)
	Mouse	Serum	LC/MS	Palmitoyl, oleoyl, myristoyl, palmitoleoyl carnitine	Elevated	(21)
	Mouse	Serum	LC/MS	Palmitoyl, oleoyl carnitine	Elevated	(22)
	Mouse	Serum	LC/MS	Palmitoyl carnitine	Elevated	(23)
	Human	Plasma	LC/MS	Palmitoyl, linoleoyl, oleoyl carnitine	No change from healthy patients	(20)
	Human	Serum	LC/MS	Palmitoyl, oleoyl, myristoyl, palmitoleoyl carnitine	Elevated	(24)
	Rat	Serum	GC/MS	*Fatty acids: O*leic acid, vaccenic acid, linoleic acid, eicosatrienoic acid, arachidonic acid, eicosapentaenoic acid, docosahexaenoic acid, myristic acid, palmitic acid, palmitoleic acid, margaric acid, stearic acid, α-linolenic acid, arachidic acid	Elevated	(25)
	Rat	Plasma	NMR	Unspecified lipid	Decreased	(13)
	Mouse	Liver	NMR	Triglycerides, monounsaturated fatty acids	Elevated	(12)
				Polyunsaturated fatty acids	Decreased	
		Plasma		Triglycerides	Elevated	
	Mouse	Serum	LC/MS	Triglycerides, free fatty acids	Elevated	(19)
	Mouse	Serum	LC/MS	Triglycerides, free fatty acids	Elevated	(22)
Citric acid cycle	Rat	Urine	NMR	2-oxoglutarate, citrate, succinate	Decreased	(13)
	Rat	Urine	NMR, LC/MS	2-oxoglutarate, citrate, succinate	Decreased	(16)
	Rat	Liver	CE/TOFMS	Citrate	Elevated	(17)
				Malate, succinate	Decreased	

Pathway	Model system	Matrix	Analytical platform	Metabolites	Directionality	Ref
	Rat	Urine	LC/MS, GC/MS	Isocitrate, aconitate, oxaloacetate	Decreased	In-house
	Human	Urine	NMR	Citrate	Decreased	(14)
Glycogen turnover	Mouse	Liver	UV/Vis	Glycogen	Decreased	(26)
		Blood		Glucose	Peak at 2 h followed by decline	
	Mouse	Liver	NMR	Glycogen, glucose	Decreased	(12)
		Plasma		Glucose	Elevated	
	Rat	Urine	NMR, LC/MS	Glucose	Decreased	(16)
	Rat	Liver		Glycogen	Decreased	
		Serum		Glucose		
Amino acid	Mouse	Liver	NMR	Alanine, isoleucine, leucine, lysine, valine, phenylalanine, tyrosine	Elevated	(12)
	Rat	Plasma	NMR	Isoleucine	Elevated	(13)
	Pig	Serum	NMR	Isoleucine, tyrosine, phenylalanine	Elevated	(27)
				Valine	Decreased	
	Human	Plasma	NMR	3-hydroxyisovalerate, isoleucine, acetylglycine, glutamine, isobutyrate, phenylalanine	Elevated	(14)
GSH and sulfur amino acid metabolism	Mouse	Liver	CE/TOFMS	Spermine, hypotaurine, S-adenosylmethionine, glycine, glutamine, spermidine, cysteine, glutamate, taurine	Decreased	(17)
	Rat	Urine	NMR	Taurine	Elevated	(13)
	Rat	Urine	NMR, LC/MS	Trigonelline	Decreased	(16)
				S-adenosylmethionine		
				Taurine		
	Rat	Urine	NMR	5-oxoproline	Increased	(28)
	Mouse	Liver	CE/TOFMS	Methionine, S-adenosylhomocysteine, ophthalmic acid	Elevated	(17)
	Rat	Liver	LC/MS, GC/MS	Taurine, hypotaurine	Decreased	(29)
				Ophthalmic acid, 5-oxoproline, γ-glutamyl-2-aminobutyrate	Increased	
Phospholipid turnover	Mouse	Liver	NMR	All phospholipid species, arachidonic acid	Decreased	(12)
				Choline, phosphocholine	Elevated	
Bile acids	Rat	Plasma	LC/MS, GC/MS	*Glycine conjugated bile acids:* Glycocholate, glycochenodeoxycholate	Elevated	(29)
				Taurine conjugated bile acids: Taurocholate, taurochenodeoxycholate	Decreased	
	Human	Serum	LC/MS	Glycodeoxycholic acid	Increased	(30)
Others	Rat	Plasma	NMR	Trimethylamine, creatinine	Elevated	(13)
	Rat	Urine	NMR	Allantoin, hippurate, creatinine, trimethylamine *N*-oxide	Decreased	(13)

Pathway	Model system	Matrix	Analytical platform	Metabolites	Directionality	Ref
	Rat	Urine	NMR, LC/MS	Trimethylamine *N*-oxide, dimethylamine, hippurate, glycine, N,N-dimethylglycine, N-isovalerylglycine, betaine, *trans*-aconitate, pipecolinate, ferulic acid	Decreased	(16)
				Creatine, acetate		
	Human	Urine	NMR	Hippurate	Decreased	(14)
				3-chlorotyrosine, glutarate	Elevated	
		Plasma		Acetone, acetate, ethanol	Elevated	
	Rat	Urine	LC/MS, GC/MS	Hippurate, pantothenate, phenylacetylglycine, pipecolinate, ferulic acid sulfate	Decreased	In-house
				Indoxysulfuric acid, pyrocatechol sulfate	Elevated	

SUPPLEMENTAL TABLE S7. List of proteins known to be covalently adducted by APAP. Proteins that are also glutathionylated in our dataset are listed in bold.

Protein	Reference
2,4-Dienoyl-CoA reductase	(31)
3-Hydroxyanthranilate 3,4-dioxygenase	(31)
Aldehyde dehydrogenase	(31, 32)
Annexin A2	
Argininosuccinate synthetase	(33)
Sulfotransferase (aryl sulfotransferase)	(31)
ATP synthase (ATP synthetase) α subunit	(31)
Calreticulin precursor	(34)
Carbomoyl-phosphate synthase (carbamyl phosphate synthetase-I)	(32)
Carbonic anhydrase III	(31)
Formimidoyltransferase cyclodeaminase	
Glutamate dehydrogenase	(32)
Glutamine synthetase	(32)
Glutathione peroxidase	(31)
Glutathione *S*-transferase π	(31)
Glyceraldehyde-3-phosphate dehydrogenase	(35)
Glycine amidinotransferase, mitochondrial	
Glycine *N*-methyl transferase	(31)
Lamin A	(32)
Methionine adenosyl transferase	(31)
Microsomal glutathione *S*-transferase	(33)
N-10-formyl tetrahydrofolate dehydrogenase	(32)
Osteoblast-specific factor 3	(31)
Peroxiredoxin 3, mouse (housekeeping protein)	(31)
Peroxiredoxin 6	
Protein deglycase DJ-1	
Proteasome subunit C8	(31)
Protein disulfide isomerase (thiol:protein disulfide oxidoreductase)	(34)
Protein synthesis initiation factor 4A	(31)
Pyrophosphatase	(31)
Ribophorin I	(33)
Selenium-binding protein 1 (acetaminophen-binding protein)	(31, 32)
Sorbitol dehydrogenase	(31)
Thioether S-methyltransferase	(31)
Tropomyosin 5	(31)
Urate oxidase	(31)
Voltage-dependent anion channel 2	

N.B. Names in parentheses refer to the synonymous protein name reported in the original publication.

Supplemental References

1. Robinson KM, Janes MS, Pehar M, Monette JS, Ross MF, Hagen TM, Murphy MP, et al. Selective fluorescent imaging of superoxide in vivo using ethidium-based probes. Proc Natl Acad Sci U S A 2006;103:15038-15043.
2. Hornak V, Abel R, Okur A, Strockbine B, Roitberg A, Simmerling C. Comparison of multiple Amber force fields and development of improved protein backbone parameters. Proteins 2006;65:712-725.
3. Dickson CJ, Madej BD, Skjevik AA, Betz RM, Teigen K, Gould IR, Walker RC. Lipid14: The Amber Lipid Force Field. J Chem Theory Comput 2014;10:865-879.
4. Essmann U, Perera L, Berkowitz ML, Darden T, Lee H, Pedersen LG. A smooth particle mesh Ewald method. The Journal of Chemical Physics 1995;103:8577-8593.
5. Van Der Spoel D, Lindahl E, Hess B, Groenhof G, Mark AE, Berendsen HJ. GROMACS: fast, flexible, and free. J Comput Chem 2005;26:1701-1718.
6. Milacic M, Haw R, Rothfels K, Wu G, Croft D, Hermjakob H, D'Eustachio P, et al. Annotating cancer variants and anti-cancer therapeutics in reactome. Cancers (Basel) 2012;4:1180-1211.
7. Su D, Gaffrey MJ, Guo J, Hatchell KE, Chu RK, Clauss TR, Aldrich JT, et al. Proteomic identification and quantification of S-glutathionylation in mouse macrophages using resin-assisted enrichment and isobaric labeling. Free Radic Biol Med 2014;67:460-470.
8. Go YM, Roede JR, Orr M, Liang Y, Jones DP. Integrated redox proteomics and metabolomics of mitochondria to identify mechanisms of cd toxicity. Toxicol Sci 2014;139:59-73.
9. Leichert LI, Gehrke F, Gudiseva HV, Blackwell T, Ilbert M, Walker AK, Strahler JR, et al. Quantifying changes in the thiol redox proteome upon oxidative stress in vivo. Proc Natl Acad Sci U S A 2008;105:8197-8202.
10. Israelson A, Abu-Hamad S, Zaid H, Nahon E, Shoshan-Barmatz V. Localization of the voltage-dependent anion channel-1 Ca2+-binding sites. Cell Calcium 2007;41:235-244.
11. De Stefani D, Bononi A, Romagnoli A, Messina A, De Pinto V, Pinton P, Rizzuto R. VDAC1 selectively transfers apoptotic Ca2+ signals to mitochondria. Cell Death Differ 2012;19:267-273.
12. Coen M, Lenz EM, Nicholson JK, Wilson ID, Pognan F, Lindon JC. An integrated metabonomic investigation of acetaminophen toxicity in the mouse using NMR spectroscopy. Chem Res Toxicol 2003;16:295-303.
13. Fukuhara K, Ohno A, Ando Y, Yamoto T, Okuda H. A 1H NMR-based metabolomics approach for mechanistic insight into acetaminophen-induced hepatotoxicity. Drug Metab Pharmacokinet 2011;26:399-406.
14. Kim JW, Ryu SH, Kim S, Lee HW, Lim MS, Seong SJ, Yoon YR, et al. Pattern recognition analysis for hepatotoxicity induced by acetaminophen using plasma and urinary 1H NMR-based metabolomics in humans. Anal Chem 2013;85:11326-11334.
15. Fannin RD, Russo M, O'Connell TM, Gerrish K, Winnike JH, Macdonald J, Newton J, et al. Acetaminophen dosing of humans results in blood transcriptome and metabolome changes consistent with impaired oxidative phosphorylation. Hepatology 2010;51:227-236.
16. Sun J, Schnackenberg LK, Holland RD, Schmitt TC, Cantor GH, Dragan YP, Beger RD. Metabonomics evaluation of urine from rats given acute and chronic doses of acetaminophen using NMR and UPLC/MS. J Chromatogr B Analyt Technol Biomed Life Sci 2008;871:328-340.

17. Soga T, Baran R, Suematsu M, Ueno Y, Ikeda S, Sakurakawa T, Kakazu Y, et al. Differential metabolomics reveals ophthalmic acid as an oxidative stress biomarker indicating hepatic glutathione consumption. J Biol Chem 2006;281:16768-16776.
18. Bhattacharyya S, Pence L, Beger R, Chaudhuri S, McCullough S, Yan K, Simpson P, et al. Acylcarnitine profiles in acetaminophen toxicity in the mouse: comparison to toxicity, metabolism and hepatocyte regeneration. Metabolites 2013;3:606-622.
19. Chen C, Krausz KW, Shah YM, Idle JR, Gonzalez FJ. Serum metabolomics reveals irreversible inhibition of fatty acid beta-oxidation through the suppression of PPARalpha activation as a contributing mechanism of acetaminophen-induced hepatotoxicity. Chem Res Toxicol 2009;22:699-707.
20. McGill MR, Li F, Sharpe MR, Williams CD, Curry SC, Ma X, Jaeschke H. Circulating acylcarnitines as biomarkers of mitochondrial dysfunction after acetaminophen overdose in mice and humans. Arch Toxicol 2014;88:391-401.
21. Yu J, Jiang YS, Jiang Y, Peng YF, Sun Z, Dai XN, Cao QT, et al. Targeted metabolomic study indicating glycyrrhizin's protection against acetaminophen-induced liver damage through reversing fatty acid metabolism. Phytother Res 2014;28:933-936.
22. Bi H, Li F, Krausz KW, Qu A, Johnson CH, Gonzalez FJ. Targeted Metabolomics of Serum Acylcarnitines Evaluates Hepatoprotective Effect of Wuzhi Tablet (Schisandra sphenanthera Extract) against Acute Acetaminophen Toxicity. Evid Based Complement Alternat Med 2013;2013:985257.
23. Patterson AD, Shah YM, Matsubara T, Krausz KW, Gonzalez FJ. Peroxisome proliferator-activated receptor alpha induction of uncoupling protein 2 protects against acetaminophen-induced liver toxicity. Hepatology 2012;56:281-290.
24. Bhattacharyya S, Yan K, Pence L, Simpson PM, Gill P, Letzig LG, Beger RD, et al. Targeted liquid chromatography-mass spectrometry analysis of serum acylcarnitines in acetaminophen toxicity in children. Biomark Med 2014;8:147-159.
25. Xiong YH, Xu Y, Yang L, Wang ZT. Gas chromatography-mass spectrometry-based profiling of serum fatty acids in acetaminophen-induced liver injured rats. J Appl Toxicol 2014;34:149-157.
26. Hinson JA, Mays JB, Cameron AM. Acetaminophen-induced hepatic glycogen depletion and hyperglycemia in mice. Biochem Pharmacol 1983;32:1979-1988.
27. Newsome PN, Henderson NC, Nelson LJ, Dabos C, Filippi C, Bellamy C, Howie F, et al. Development of an invasively monitored porcine model of acetaminophen-induced acute liver failure. BMC Gastroenterol 2010;10:34.
28. Ghauri FY, McLean AE, Beales D, Wilson ID, Nicholson JK. Induction of 5-oxoprolinuria in the rat following chronic feeding with N-acetyl 4-aminophenol (paracetamol). Biochem Pharmacol 1993;46:953-957.
29. Yamazaki M, Miyake M, Sato H, Masutomi N, Tsutsui N, Adam KP, Alexander DC, et al. Perturbation of bile acid homeostasis is an early pathogenesis event of drug induced liver injury in rats. Toxicol Appl Pharmacol 2013;268:79-89.
30. Woolbright BL, McGill MR, Staggs VS, Winefield RD, Gholami P, Olyaee M, Sharpe MR, et al. Glycodeoxycholic acid levels as prognostic biomarker in acetaminophen-induced acute liver failure patients. Toxicol Sci 2014;142:436-444.
31. Qiu Y, Benet LZ, Burlingame AL. Identification of the hepatic protein targets of reactive metabolites of acetaminophen in vivo in mice using two-dimensional gel electrophoresis and mass spectrometry. J Biol Chem 1998;273:17940-17953.

32. Cohen SD, Pumford NR, Khairallah EA, Boekelheide K, Pohl LR, Amouzadeh HR, Hinson JA. Selective protein covalent binding and target organ toxicity. Toxicol Appl Pharmacol 1997;143:1-12.
33. Zhang H, Gan J, Shu YZ, Humphreys WG. High-resolution mass spectrometry-based background subtraction for identifying protein modifications in a complex biological system: detection of acetaminophen-bound microsomal proteins including argininosuccinate synthetase. Chem Res Toxicol 2015;28:775-781.
34. Zhou L, McKenzie BA, Eccleston ED, Jr., Srivastava SP, Chen N, Erickson RR, Holtzman JL. The covalent binding of [14C]acetaminophen to mouse hepatic microsomal proteins: the specific binding to calreticulin and the two forms of the thiol:protein disulfide oxidoreductases. Chem Res Toxicol 1996;9:1176-1182.
35. Dietze EC, Schafer A, Omichinski JG, Nelson SD. Inactivation of glyceraldehyde-3-phosphate dehydrogenase by a reactive metabolite of acetaminophen and mass spectral characterization of an arylated active site peptide. Chem Res Toxicol 1997;10:1097-1103.